

Optical properties of a α -plane InGaN/GaN multiple quantum wells on r -plane sapphire substrates with different indium compositions

C. H. Chiu, S. Y. Kuo, M. H. Lo, C. C. Ke, T. C. Wang, Y. T. Lee, H. C. Kuo, T. C. Lu, and S. C. Wang

Citation: *Journal of Applied Physics* **105**, 063105 (2009); doi: 10.1063/1.3083074

View online: <http://dx.doi.org/10.1063/1.3083074>

View Table of Contents: <http://scitation.aip.org/content/aip/journal/jap/105/6?ver=pdfcov>

Published by the [AIP Publishing](#)

Articles you may be interested in

[The defect character of GaN growth on \$r\$ -plane sapphire](#)

J. Appl. Phys. **107**, 073525 (2010); 10.1063/1.3369439

[Exciton localization on basal stacking faults in a \$\alpha\$ -plane epitaxial lateral overgrown GaN grown by hydride vapor phase epitaxy](#)

J. Appl. Phys. **105**, 043102 (2009); 10.1063/1.3075596

[Improved \$\alpha\$ -plane GaN quality grown with flow modulation epitaxy and epitaxial lateral overgrowth on \$r\$ -plane sapphire substrate](#)

Appl. Phys. Lett. **92**, 231902 (2008); 10.1063/1.2942391

[Erratum: "Interfacial structure of a \$\alpha\$ -plane GaN grown on \$r\$ -plane sapphire" \[*Appl. Phys. Lett.*90, 081918 \(2007\)\]](#)

Appl. Phys. Lett. **90**, 249901 (2007); 10.1063/1.2744473

[Interfacial structure of a \$\alpha\$ -plane GaN grown on \$r\$ -plane sapphire](#)

Appl. Phys. Lett. **90**, 081918 (2007); 10.1063/1.2696309



Re-register for Table of Content Alerts

Create a profile.



Sign up today!



Optical properties of *a*-plane InGaN/GaN multiple quantum wells on *r*-plane sapphire substrates with different indium compositions

C. H. Chiu,^{1,a)} S. Y. Kuo,² M. H. Lo,¹ C. C. Ke,¹ T. C. Wang,¹ Y. T. Lee,¹ H. C. Kuo,^{1,a)} T. C. Lu,¹ and S. C. Wang¹

¹*Department of Photonics and Institute of Electro-Optical Engineering, National Chiao-Tung University, Hsinchu, Taiwan, Republic of China*

²*Department of Electronic Engineering, Chang Gung University, TaoYuan, Taiwan, Republic of China*

(Received 6 October 2008; accepted 14 January 2009; published online 24 March 2009)

A-plane In_xGa_{1-x}N/GaN (*x*=0.09, 0.14, 0.24, and 0.3) multiple-quantum-wells (MQWs) samples, with a well width of about 4.5 nm, were achieved by utilizing *r*-plane sapphire substrates. Optical quality was investigated by means of photoluminescence (PL), cathodoluminescence, and time resolved PL measurements (TRPL). Two distinguishable emission peaks were examined from the low temperature PL spectra, where the high- and low-energy peaks were ascribed to quantum wells and localized states, respectively. Due to an increase in the localized energy states and absence of quantum confined Stark effect, the quantum efficiency was increased with increasing indium composition up to 24%. As the indium composition reached 30%, however, pronounced deterioration in luminescence efficiency was observed. The phenomenon could be attributed to the high defect densities in the MQWs resulted from the increased accumulation of strain between the InGaN well and GaN barrier. This argument was verified from the much shorter carrier lifetime at 15 K and smaller activation energy for In_{0.3}Ga_{0.7}N/GaN MQWs. In addition, the polarization-dependent PL revealed that the degree of polarization decreased with increasing indium compositions because of the enhancement of zero-dimensional nature of the localizing centers. Our detailed investigations indicate that the indium content in *a*-plane InGaN/GaN MQWs not only has an influence on optical performance, but is also important for further application of nitride semiconductors. © 2009 American Institute of Physics. [DOI: 10.1063/1.3083074]

I. INTRODUCTION

InGaN-based semiconductors have been used intensively as light emitting diodes (LEDs) and laser diodes due to their wide direct band gap ranging from green to ultraviolet light.¹ However, the quantum efficiency is limited in the conventional *c*-plane polar structure due to the built-in electric field called quantum confined Stark effect (QCSE). This built-in electric field would decrease the oscillator strength of the electron-hole pairs and reduce the carrier recombination rate. Thus in highly efficient InGaN/GaN multiple quantum wells (MQWs) based devices, the InGaN well has a thickness of less than 3 nm to avoid degradation of the light emission by the QCSE. Moreover, because of the low miscibility of InN in GaN, there exists partial phase segregation within InGaN-based structures.² This partial phase segregation and composition inhomogeneity would result in exciton localization within some indium-rich regions.³ Consequently, the luminescence efficiency could be enhanced due to the effective carrier confinement in the localization states. Such exciton localization effect is influenced by the quantum well thickness, indium compositions, and doping concentration. For *c*-plane InGaN/GaN MQWs, the influence of indium compositions on the optical characteristics has been studied extensively in order to optimize InGaN/GaN MQW quantum efficiency.^{4,5}

Recently, several groups have grown samples with non-polar structures in order to eliminate the built-in electric field.⁶ Our group also reported the influence on optical properties of *a*-plane In_{0.23}Ga_{0.77}N MQWs with different well width ranging from 3 to 12 nm and we found the photoluminescence (PL) intensity decreased as the well width was increased especially for those larger than ~6–7 nm.⁷ Nonpolar InGaN/GaN MQWs containing less indium can be used to extend the light emission to the green spectral range due to the absence of QCSE, which is still a challenge for high efficiency InGaN/GaN MQW LEDs and lasers. Up to now, however, the structural and optical properties of nonpolar InGaN/GaN MQWs are still inferior compared to their mature *c*-plane grown counterpart due to much higher dislocation densities when grown on *r*-plane sapphire substrates.

In this paper, the optical properties of the *a*-plane [11 $\bar{2}$ 0] In_xGa_{1-x}N/GaN MQWs on *r*-plane sapphire substrates with different indium compositions (*x* ~ 9%, 14%, 24%, and 30% with well width of ~4.5 nm) have been investigated by means of PL, cathodoluminescence (CL), and time resolved PL measurements (TRPL). The influence of indium composition on luminescence efficiency in InGaN/GaN MQWs as well as polarization properties is discussed.

II. EXPERIMENT

The 1.5- μ m-thick *a*-plane [11 $\bar{2}$ 0] bulk GaN was grown by Aixtron 2400G3 multiwafer low pressure metal-organic chemical vapor deposition (LP-MOCVD) on *r*-plane sap-

^{a)}Authors to whom correspondence should be addressed. Electronic addresses: chchiu.eo95g@nctu.edu.tw and hckuo@faculty.nctu.edu.tw.

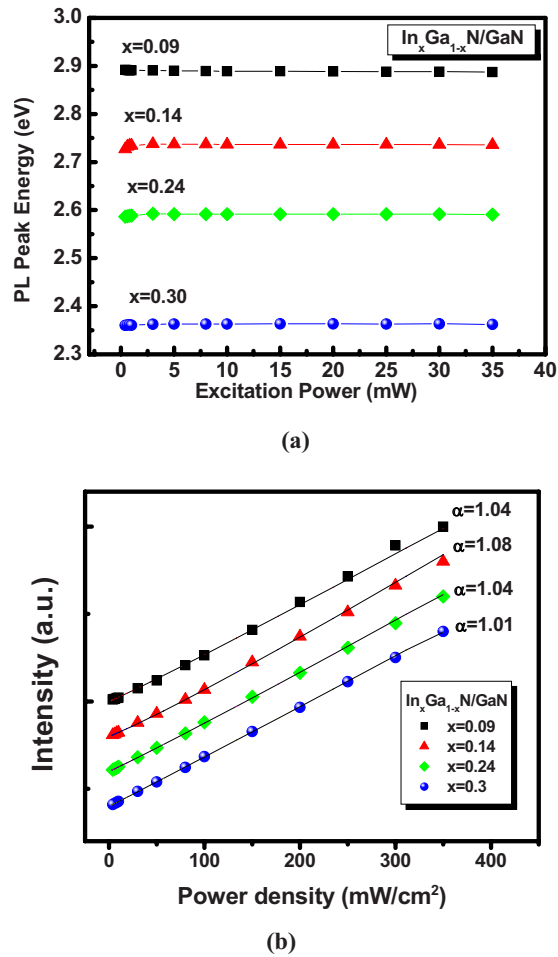


FIG. 1. (Color online) The power-dependent PL measurement of the four samples, (a) the emission wavelength vs the pumping power and (b) the PL intensity vs the pumping density and fitted based on the relation $I \sim P^\alpha$.

phire substrates using conventional two-step growth technique.⁸ Four samples with identical structure and 10 pairs of 4.5-nm-thick InGaN well/18-nm-thick GaN barrier MQWs were under the same growth condition except for the growth temperature. The growth temperature for the four samples was controlled at 870, 850, 830, and 810 °C, respectively. The anisotropic strain within nonpolar structures will result in more complex Poisson ratio. After high resolution x-ray diffraction measurements, we could estimate the indium compositions to be ~9%, 14%, 24%, and 30% for InGaN/GaN MQW samples.⁹

III. RESULTS AND DISCUSSIONS

First, the power-dependent PL measurement of the four samples at room temperature was performed as shown in Fig. 1(a). All samples were excited by a 325 nm He–Cd laser with an excitation power of 35 mW and the emitted luminescence light was collected through a 0.32 m spectrometer with a charge-coupled device detector. The focused spot size of the laser was estimated to be about 200 μm in diameter. As illustrated in Fig. 1(a), the room-temperature PL peak emission energy of InGaN/GaN MQWs decreases from 2.89 to

2.36 eV through all samples despite various excitation power. Furthermore, all samples show extremely small shift in emission peak energy with increasing the pumping power from 0.4 to 35 mW. The integrated PL intensity was fitted based on the relation $I \sim P^\alpha$, where I is the integrated PL intensity, P is the excitation power density, and α is the power index. Shown in Fig. 1(b) are the fitting results of integrated PL intensity. While increasing indium composition from 9% to 30%, the α factors of the four samples were 1.04, 1.08, 1.04, and 1.01, respectively. From the negligible PL peak emission energy shift and nearly identical α factors, it is suggested that the QCSE is extremely small or absent in our *a*-plane InGaN/GaN MQWs with indium compositions varying from ~9% to 30%.

Figure 2 shows the temperature-dependent PL spectra taken from 20 to 300 K at an excitation power of 30 mW. At low temperature, the spectra exhibit a multiple-peak feature and can be decomposed into two dominant peaks, higher-energy emission (denoted by P_H) and lower-energy emission (denoted by P_L). As the temperature increases, the peak intensity of P_H quenches quickly and the P_L becomes dominant for all InGaN/GaN MQW samples. It is suggested that P_H is a MQW-related emission and P_L is from the deep localized states. This argument will be discussed by TRPL results later.

To further clarify the PL mechanism, the 20 K PL spectra were decomposed into a sum of two Gaussian curves, P_H and P_L , mentioned above. Fitting results are shown in Figs. 3(a) and 3(b) for four InGaN/GaN MQWs samples. In Fig. 3(a), we can clearly see that both emission peak energies decreased as the indium concentration increased. On the other hand, the peak emission difference seems to be gradually increased from 240 to 290 meV. The difference between these two emission peaks suggests that the higher the indium compositions, the deeper the localized centers existing in InGaN/GaN MQWs. Thus the carrier would be easier to migrate to the lowest state in the high indium concentration sample. This phenomenon could explain the enhanced peak intensity ratio of the P_L to P_H peaks as indium concentration increased. Figure 3(b) summarizes the full width at half maximum (FWHM) of these two peaks for all samples at 20 K. It is noteworthy that the FWHM of the P_L peaks keeps constant in all samples while that of the P_H peak increases linearly with indium compositions. This broadening phenomenon of the P_L peak indicates that an increasing degree of compositional and structural disorders with increasing indium concentration deteriorates the crystal quality in the quantum wells, which has been extensively reported.

In addition, the evolution with temperature of the peak shift of P_L peak for the four samples investigated here is given in Fig. 3(c), where the peak positions at 20 K are the reference. The peak shift of PL varies as a function of temperature from 20 to 300 K and exhibits a continuous redshift. With increasing indium composition, the total redshift value at room temperature in Fig. 3(c) reduced from 85 to 30 meV. The smaller redshift may be due to more localization centers with higher indium compositions.¹⁰ Thus the confinement of the localization would be improved as we increase indium composition, which is consistent with the result of Fig. 3(c).

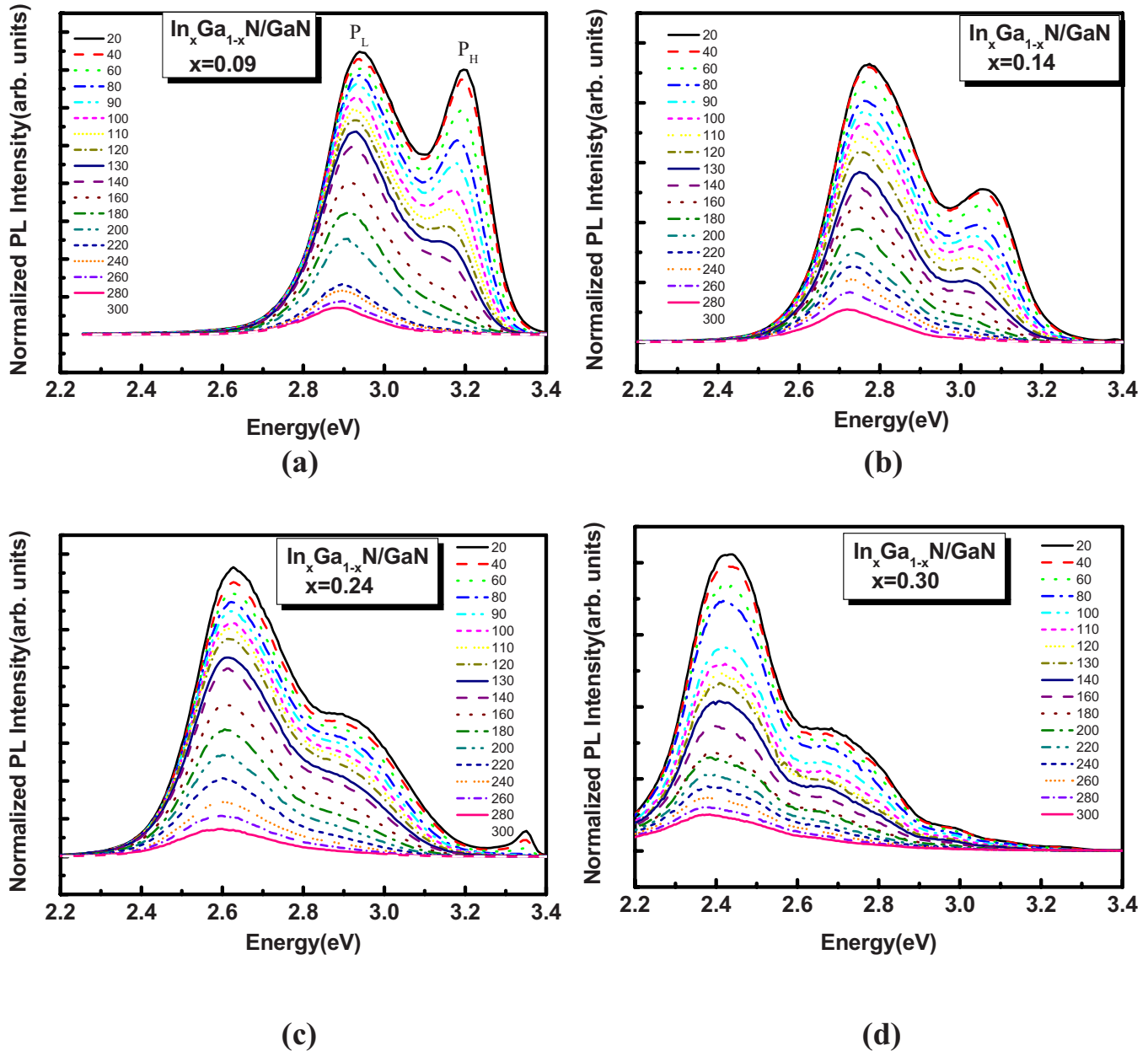


FIG. 2. (Color online) The PL emission spectra under temperature varied from 1 to 300 K. (a)–(d) imply the samples with In compositions varied from 9% to 30%.

It has been studied that the carrier could receive activation energy to thermalize from the potential minima, the radiative or localized centers, to nonradiative or delocalized centers as the temperature is increased.¹¹ Therefore, it is expected that the deeper localization with better confinement should have larger activation energy. In order to further verify that, the experimental temperature-dependent PL data were fitted by Arrhenius equation to investigate the carrier behavior during the thermal processes,¹²

$$I(T) = \frac{I_0}{1 + A^* \exp\left(-\frac{E_a}{K_B T}\right) + B^* \exp\left(-\frac{E_b}{K_B T}\right)},$$

where $I(T)$ is the temperature-dependent PL intensity, I_0 is the PL intensity at 20 K, K_B is Boltzmann's constant, A and

B are the rate constants, and E_a and E_b are the activation energies for two different nonradiative channels, which can be distinguished for the low temperature and high temperature regions.¹³ The fitted activation energy of the four samples is listed in Fig. 4. As expected, the activation energy gradually increases and reaches the maximum value of 110 meV when indium composition is 24%. It has been reported that several defects such as V-defects, stacking faults, and dislocations will be formed in the MQWs during sample growth, resulting in deterioration in the structural and optical properties of MQWs.¹⁴ Consequently, as indium composition is continuously increased, large numbers of defects may exist in our samples. Photogenerated carriers will be easily trapped by high-density nonradiative centers before they reached the potential minimum. Thus the activation energy

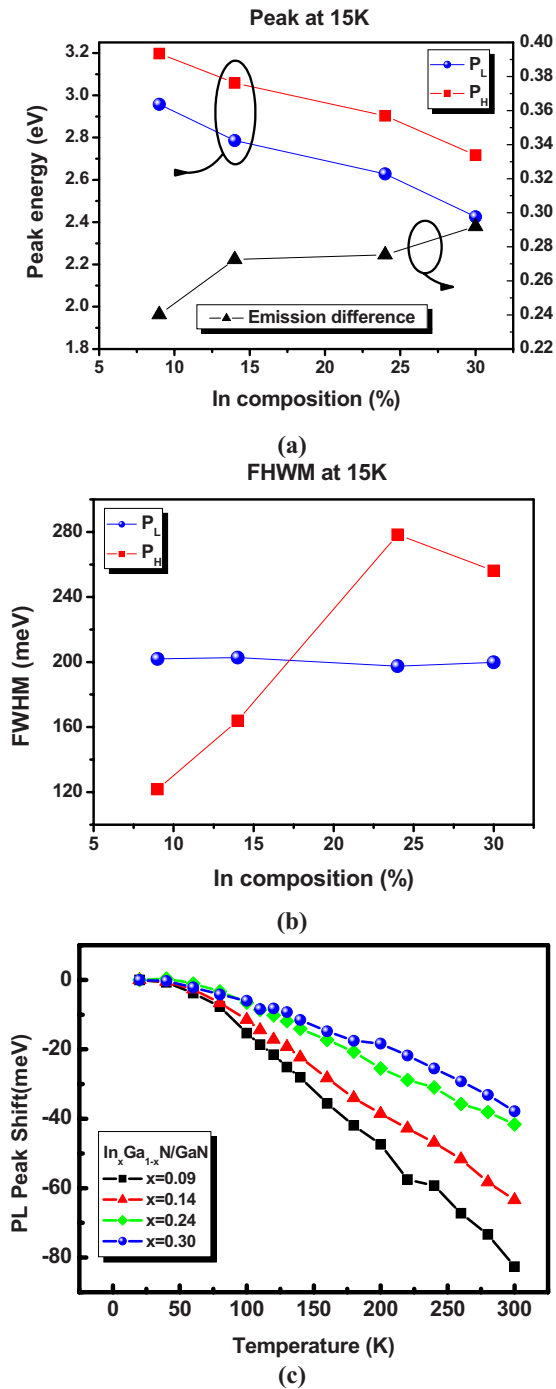


FIG. 3. (Color online) The summary of the temperature-dependent PL results of the four samples with different In compositions. (a) shows the emission wavelength and difference between high and low emission peaks, (b) shows the FWHM of the dominate and high energy peaks, and (c) shows the dominate wavelength shift from 20 to 300 K.

of InGa_xN_{1-x}/Ga_xN_{1-x} MWQs with 30% indium composition lowered to 85 meV.

Furthermore, the TRPL measurements at 15 K were performed to investigate the effects of indium compositions on the carrier recombination mechanism as shown in Fig. 5. The experimental data exhibit a nonexponential called stretched exponential decay shape, which is a characteristic of the emission from disorder quantum structures such as the localized states.^{15,16} The TRPL results can be fitted by the stretched exponential decay shape,

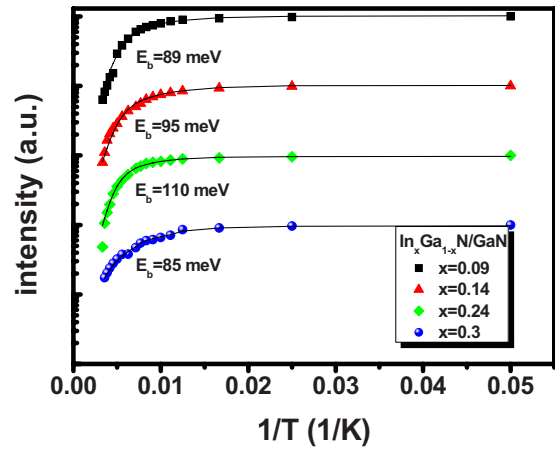


FIG. 4. (Color online) The normalized PL intensity plotted as a function of $1/T$ for the samples with different In compositions. The symbols stand for the measurement results and the solid line means the fitted curve of the four samples. The number labeled near the curves represents the fitted activation energies.

$$I(t) = I_1(0)\exp\left(-\frac{t}{\tau_1}\right) + I_2(0)\exp\left(-\left(\frac{t}{\tau_2}\right)^\beta\right),$$

where $I(t)$ is the PL intensity at time t , β is the dimensionality of the localized centers, and τ_1 and τ_2 represent the initial lifetimes of the carriers. Normally, the fast decay term τ_1 is used represent τ_{PL} since the PL intensity is limited by the fast decay component,¹⁷ so we labeled all fitted τ_1 near the curves. From Fig. 5, we found that the fitted lifetime of τ_1 equals 418, 405, 391, and 289 ps in P_L and 491, 457, 416, and 375 ps in P_H for indium composition changing from 9% to 30%. It first shows that the P_L peaks have shorter lifetime than P_H peaks in all samples. The results of shorter lifetime of P_L coincide with the stronger emission intensity than the P_H showing in the inset of Fig. 5, since it corresponds to a higher recombination rate at low temperature. Therefore, it is reasonable to assign the P_H and P_L to MQWs-related and localized states emission, respectively. Second, the carrier lifetime of P_L slightly decreased as indium composition is

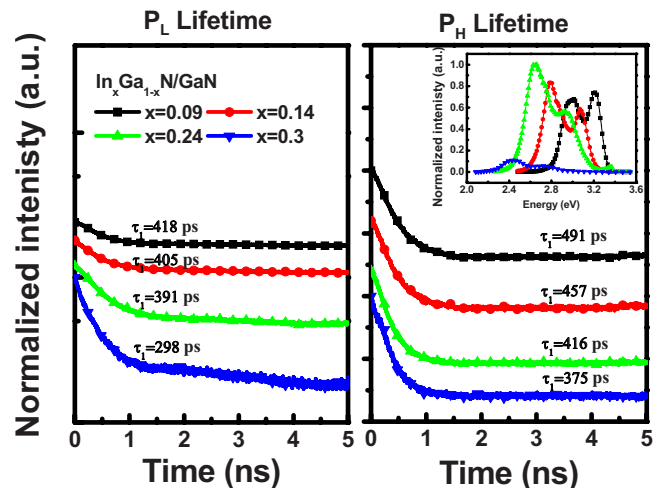


FIG. 5. (Color online) The measured lifetime of P_H and P_L peaks for samples with different In compositions at 15 K. The inset shows the measured PL spectra of the four samples.

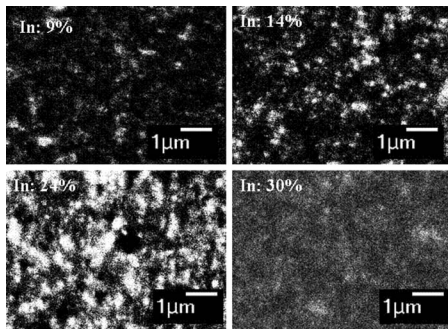


FIG. 6. Top view cathodoluminescence images of *a*-plane InGaN/GaN MQWs with different In compositions at corresponding dominate emission peak wavelengths.

below 24%, but dropped from 391 to 289 ps as the indium composition increased from 24% to 30%. As expected, the integrated PL intensity is reversely proportional to the carrier lifetime as x is below 24%. However, contrary to our expectations, the PL intensity of the sample with 30% indium composition drops to about only 1/5 compared to the luminescence intensity of the sample with 24% indium composition. It is known that the nonradiative lifetime is much shorter than radiative lifetime, so the appreciable reduction in lifetime and PL intensity revealed the fact of large number of nonradiative centers in the sample with 30% indium composition.¹⁸ For the InGaN alloy system, nanoscale fluctuations in the local indium concentration are expected to form easily and produce more disorder. Therefore, the carrier recombination is probably determined by another nonradiative mechanism. Further evidence of indium phase segregation by CL image mapping will be discussed later. In addition, the lifetime extracted from the *a*-plane samples under 15 K is much shorter (<0.5 ns) than that of *c*-plane MQWs reported in previous literature [~ 5.8 ns (Ref. 6)].

Taking luminescence efficiency into consideration, CL mapping measurement could provide constructive information. Figure 6 shows the CL images of the four samples with a JEOL-JSM 6500 scanning electron microscope under an accelerating voltage of 15 kV at room temperature. The four images were scanned at monitoring the respective peak emission wavelength. At first glance, the nonuniform emission patterns are observed from all samples, which were mainly due to the indium composition fluctuation and the phase separation.¹⁹ Interestingly, it is found that, with the increase in indium composition, the emission area and intensity gradually increase and, hence, exhibit a better uniformity emission pattern, except for the sample with highest indium compositions. It suggests that $\text{In}_{0.24}\text{Ga}_{0.76}\text{N}/\text{GaN}$ MQWs sample has relatively higher luminescence efficiency among these samples.

In order to demonstrate the optical characteristic of non-polar MQWs, the polarization-dependent PL measurement was taken. Shown in Fig. 7 is the polarization ratio plotted as the function of indium compositions at 20 and 300 K. The degree of polarization (DOP) is defined as $\text{DOP} = \frac{I_{\perp} - I_{\parallel}}{I_{\perp} + I_{\parallel}}$, where I_{\perp} and I_{\parallel} are PL intensities represented for $E \perp C$ and $E \parallel C$. As we can see from Fig. 7, DOP decreased as temperature increased in all samples. This feature might be

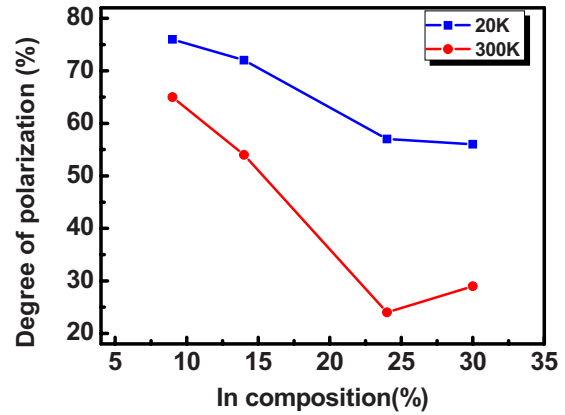


FIG. 7. (Color online) The DOP plotted as the function of In compositions at 20 and 300 K, respectively.

explained that carriers in these samples have sufficient energy to be thermally distributed to the other local minimums states. Accordingly, the DOP decreases with increasing temperature.²⁰ In addition, DOP decreases with increasing indium composition. The decrease in the DOP might be attributed to the enhancement of zero-dimensional nature of the localizing radiative centers, most of which are the dotlike indium-rich region in MQWs. Therefore, with increasing indium compositions, more carriers would be confined at localization centers which then reduces the DOP.²¹

IV. CONCLUSION

In summary, the optical properties of the samples grown by LP-MOCVD on *r*-plane sapphire with different indium compositions ranging from 9% to 30% were investigated. All samples manifest two distinguishable emission peaks, where the high-energy and low-energy peaks were attributed to quantum wells and localized states, respectively. No obvious emission peak shift is observed from the power-dependent PL measurement for all samples, which is the evidence to the absence of QCSE. While the indium composition was raised to 24%, the increase in activation energy and decrease in carrier lifetime implied that more and deeper localized states formed and contribute to better quantum efficiency. However, the MQWs sample with 30% indium composition reveals dramatic reduction in activation energy and lifetime at low temperature. The observation implied the large numbers of defects formed in high indium samples, consistent with earlier literatures. Besides, from the polarization-dependent PL measurement, the DOP reduced in increasing temperatures and indium compositions. The phenomenon might be related to the enhancement in zero-dimensional nature of the localized radiative centers. These results suggest that $\text{In}_{0.24}\text{Ga}_{0.76}\text{N}/\text{GaN}$ MQWs sample has the relatively higher luminescence efficiency among these samples, which provides useful guidance for the fabrication of high efficiency LEDs with *a*-plane InGaN/GaN MQW structures.

ACKNOWLEDGMENTS

The authors thank Professor J. L. Shen of Chung Yuan Christian University for useful discussion. The work was supported by the MOE ATU program and in part by the National Science Council in Taiwan under Contract Nos. NSC 95-2120-M-009-008, NSC 95-2752-E-009-007-PAE, and NSC 95-2221-E-009-282, and Epistar Co. Ltd. in Taiwan.

- ¹S. Nakamura and G. Fasol, *The Blue Laser Diode* (Springer, Berlin, 1997).
- ²I. Ho and G. B. Stringfellow, *Appl. Phys. Lett.* **69**, 2701 (1996).
- ³R. W. Martin, P. G. Middleton, K. P. O'Donnell, and W. Van Der Stricht, *Appl. Phys. Lett.* **74**, 263 (1999).
- ⁴H. C. Yang, P. F. Kuo, T. L. Lin, Y. F. Chen, K. H. Chen, L. C. Chen, and J.-I. Chyi, *Appl. Phys. Lett.* **76**, 3712 (2000).
- ⁵A. Sasaki, S. I. Shibakawa, Y. Kawakami, K. Nishizuka, Y. Narukawa, and T. Mukai, *Jpn. J. Appl. Phys., Part 1* **45**, 8719 (2006). In_xGa_{1-x}N/GaN.
- ⁶P. Waltereit, O. Brandt, A. Trampert, H. T. Grahn, J. Menniger, M. Ramsteiner, M. Reiche, and K. H. Ploog, *Nature (London)* **406**, 865 (2000).
- ⁷T. S. Ko, T. C. Lu, T. C. Wang, M. H. Lo, J. R. Chen, R. C. Gao, H. C. Kuo, and S. C. Wang, *Appl. Phys. Lett.* **90**, 181122 (2007).
- ⁸T. C. Wang, T. S. Ko, T. C. Lu, H. C. Kuo, R. C. Gao, J. D. Tsay, and S. C. Wang, *Phys. Status Solidi* **5**, (c), 2161 (2008).
- ⁹S. Nakamura, G. Fasol, and S. J. Pearton, *The Blue Laser Diode the Complete Story*, 2nd ed. (Springer, Berlin, 2000).
- ¹⁰S. F. Chichibu, T. Azuhata, T. Kitamura, Y. Ishida, H. Okumura, H. Nakanishi, T. Sota, and T. Mukai, *J. Vac. Sci. Technol. B* **19**, 2177 (2001).
- ¹¹Y. H. Cho, G. H. Gainer, A. J. Fischer, J. J. Song, S. Keller, U. K. Mishra, and S. P. DenBaars, *Appl. Phys. Lett.* **73**, 1370 (1998).
- ¹²A. Yasan, R. McClintock, K. Mayes, D. H. Kim, P. Kung, and M. Razeghi, *Appl. Phys. Lett.* **83**, 4083 (2003).
- ¹³M. Leroux, N. Grandjean, B. Beaumont, G. Nataf, F. Semond, J. Massies, and P. Gibart, *J. Appl. Phys.* **86**, 3721 (1999).
- ¹⁴H. K. Cho, J. Y. Lee, C. S. Kim, and G. M. Yang, *J. Electron. Mater.* **30**, 1348 (2001).
- ¹⁵X. Chen, B. Henderson, and K. P. O'Donnell, *Appl. Phys. Lett.* **60**, 2672 (1992).
- ¹⁶T. Onuma, T. Koyama, A. Chakraborty, M. Mclaurin, B. A. Haskell, P. T. Fini, S. Keller, S. P. DenBaars, J. S. Speck, S. Nakamura, U. K. Mishra, T. Sota, and S. F. Chichibu, *J. Vac. Sci. Technol. B* **25**, 1524 (2007).
- ¹⁷T. Onuma, A. Chakraborty, B. A. Haskell, S. Keller, S. P. DenBaars, J. S. Speck, S. Nakamura, and U. K. Mishra, *Appl. Phys. Lett.* **86**, 151918 (2005).
- ¹⁸S. F. Chichibu, T. Onuma, T. Aoyama, K. Nakajima, P. Ahmet, T. Chikyow, T. Sota, S. P. DenBaars, S. Nakamura, T. Kitamura, Y. Ishida, and H. Okumura, *J. Vac. Sci. Technol. B* **21**, 1856 (2003).
- ¹⁹P. Waltereit, O. Brandt, M. Ramsteiner, A. Trampert, H. T. Grahn, J. Menniger, M. Reiche, and K. H. Ploog, *J. Cryst. Growth* **227–228**, 437 (2001).
- ²⁰M. Kubota, K. Okamoto, T. Tanaka, and H. Ohta, *Appl. Phys. Lett.* **92**, 011920 (2008).
- ²¹T. Koyama, T. Onuma, H. Masui, A. Chakraborty, B. A. Haskell, S. Keller, U. K. Mishra, J. S. Speck, S. Nakamura, and S. P. DenBaars, *Appl. Phys. Lett.* **89**, 091906 (2006).